Article

Triplet State Photosensitization of Nanocrystalline Metal Oxide Electrodes by Zinc-Substituted Cytochrome *c*: Application to Hydrogen Evolution

Yeni Astuti, Emilio Palomares, Saif Ahmed Haque, and James Robert Durrant

J. Am. Chem. Soc., **2005**, 127 (43), 15120-15126• DOI: 10.1021/ja0533444 • Publication Date (Web): 08 October 2005

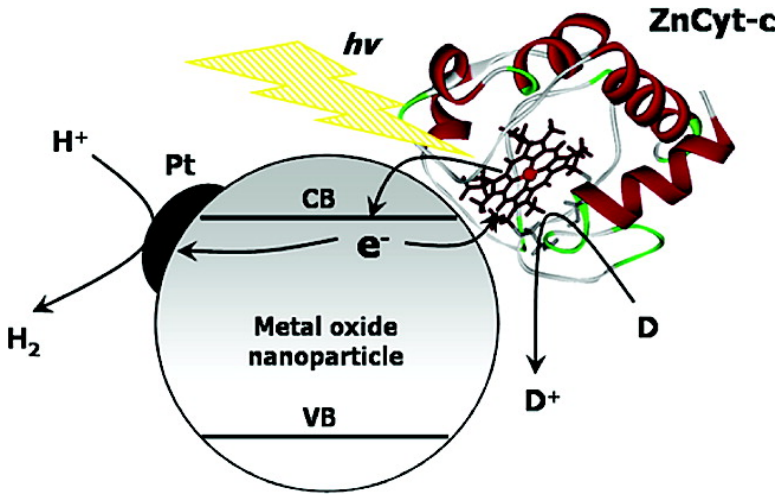

More About This Article

Additional resources and features associated with this article are available within the HTML version:

- Supporting Information
- Links to the 3 articles that cite this article, as of the time of this article download
- Access to high resolution figures
- Links to articles and content related to this article
- Copyright permission to reproduce figures and/or text from this article

View the Full Text HTML

J|A|C|S
ARTICLES
Published on Web 10/08/2005

Triplet State Photosensitization of Nanocrystalline Metal Oxide Electrodes by Zinc-Substituted Cytochrome *c*: Application to Hydrogen Evolution

Yeni Astuti,[†] Emilio Palomares,[†,‡] Saif Ahmed Haque,[†] and James Robert Durrant*[,†]

Contribution from the Department of Chemistry, Imperial College London, Exhibition Road, London SW7 2AZ, United Kingdom, and Institut de Ciència Molecular, Universitat de Valencia (IcMol-UV), C\ Dr. Moliner 50, Burjassot C.P. 46400, Valencia, Spain

Received May 23, 2005; E-mail: j.durrant@imperial.ac.uk

Abstract: The interfacing of nanostructured semiconductor photoelectrodes with redox proteins is an innovative approach to the development of artificial photosynthetic systems. In this paper, we have investigated the photoinduced electron-transfer reactions of zinc-substituted cytochrome *c*, ZnCyt-c, immobilized on mesoporous, nanocrystalline metal oxide electrodes. Efficient electron injection from the triplet state of ZnCyt-c is observed into TiO_2 electrodes ($t_{50\%} \sim 100$ μs) resulting in a long-lived charge-separated state (lifetime of up to 0.4 s). Further studies were undertaken as a function of electrolyte pH and metal oxide employed. Optimum yield of a long-lived charge-separated state was observed employing TiO_2 electrodes at pH 5, consistent with our previous studies of analogous dye-sensitized metal oxide electrodes. The addition of EDTA as a sacrificial electron donor to the electrolyte resulted in efficient photogeneration of molecular hydrogen, with a quantum yield per one absorbed photon of 10 $\pm$ 5%.

Introduction

The development of artificial photosynthesic systems is currently attracting strong scientific interest.[1] On the one hand, such studies are inspired by the rapid progress currently being made in elucidating the function of natural photosynthetic systems, in particular the structure and function of the water oxidation complex of photosystem II (PS II).[2,3] On the other hand, growing environmental concerns are motivating studies of innovative solar energy conversion systems, which build upon our understanding of natural photosynthesis.[4] One goal of such systems is the conversion of solar irradiation into electrical power. However, increasing interest in the potential of hydrogen as a fuel vector is motivating studies of the photolysis of water to generate hydrogen.[5−8] In pioneering studies in the 1970s, Fujishima and Honda demonstrated that photoexcitation of TiO_2 electrodes could be used to achieve such photolysis of water to molecular hydrogen and oxygen.[9] However, such photolysis was only achieved by band gap (ultraviolet) excitation of the TiO_2 electrodes, limiting the potential of such electrodes for efficient solar energy conversion. Extensive attempts to modify such electrodes to achieve the photolysis of water by visible light have only achieved limited success to date, not least because of the difficulty of interfacing a suitable water oxidation catalyst to the photoelectrode. One approach to this challenge is to target the interfacing to the photoelectrode of polypeptide-based water oxidation catalysts mimicking the water oxidation complex of PS II, employing either the natural protein or synthetic protein maquette analogues. The study reported here represents a key step toward achieving this long term objective, namely, the demonstration of efficient interfacing of a redox protein to a nanocrystalline metal oxide electrode resulting, in the presence of a suitable sacrifical electron donor, in remarkably efficient hydrogen production under visible light irradiation, as illustrated in Figure 1.

The sensitization of nanocrystalline metal oxide electrodes with molecular dyes is now well established for the photoelectrochemical conversion of solar energy to electrical power.[10−13] We and others have conducted extensive studies of interfacial electron-transfer dynamics in such systems as a function of molecular control of the interface and the correlation of these dynamics with device performance. In parallel with these studies we have also shown that it is possible to anchor to a range of redox proteins and enzymes to these mesoporous electrodes with remarkably high protein loadings (on the order of 10 nanomoles/cm^2 for 4 μm thick films).[14] Optical, electrochemical, and spectroelectrochemical studies of such films all indicate that

[†] Imperial College London.
[‡] Universitat de Valencia.

(1) Gust, D.; Moore, T. A.; Moore, A. L. *Acc. Chem. Res.* **2001**, *34*, 40−48.
(2) Ferreira, K. N.; Iverson, T. M.; Maghlaoui, K.; Barber, J.; Iwata, S. *Science* **2004**, *303*, 1831−1838.
(3) Barber, J. *Int. J. Photoenerg.* **2004**, *6*, 43−51.
(4) Pacala, S.; Socolow, R. *Science* **2004**, *305*, 968−972.
(5) Turner, J. A. *Science* **2004**, *305*, 972−974.
(6) Gratzel, M. *Nature* **2001**, *414*, 338−344.
(7) Zou, Z.; Ye, J.; Sayama, K.; Arakawa, H. *Nature* **2001**, *414*, 625−627.
(8) Melis, A.; Happe, T. *Photosynth. Res.* **2004**, *80*, 401−409.
(9) Fujishima, A.; Honda, K. *Nature* **1972**, *238*, 37−38.
(10) Durrant, J. R.; Haque, S. A. *Nat. Mater.* **2003**, *2*, 362−363.
(11) Hagfeldt, A.; Gratzel, M. *Acc. Chem. Res.* **2000**, *33*, 269−277.
(12) Durrant, J. R.; Haque, S. A.; Palomares, E. *Coord. Chem. Rev.* **2004**, *248*, 1247−1257.
(13) Gratzel, M. *J. Photochem. Photobiol., A* **2004**, *164*, 3−14.
(14) Topoglidis, E.; Campbell, C. J.; Cass, A. E. G.; Durrant, J. R. *Langmuir* **2001**, *17*, 7899−7906.

10.1021/ja0533444 CCC: $30.25

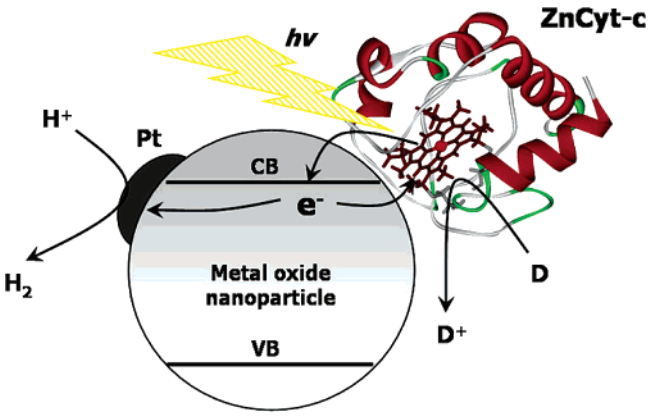

Figure 1. Schematic representation of our ZnCyt-c/metal-oxide-based artificial photosystem.

immobilized proteins retain their native conformation and redox/catalytic activities.[15−18]

Several studies have addressed the photophysical and photochemical properties of Zn-substituted cytochrome *c* (ZnCyt-c). The exchange of the iron in native Cyt-c with zinc allows the photogeneration of long-lived singlet and triplet excited states without significantly disrupting the protein conformation.[19−22] Previous studies have, for example, demonstrated photoinduced electron transfer from ZnCyt-c to plastocyanin in silica glasses and to polyanionic fullerene dendrimers in aqueous solutions.[23,24] Guo et al. have reported fluorescence quenching of the ZnCyt-c singlet excited state when the protein was immobilized on SnO_2 electrodes, assigned to electron injection into the SnO_2 conduction band.[20] We have recently extended such studies to mesoporous TiO_2 electrodes, reporting the photogeneration of a long-lived charge-separated state $(ZnCyt\text{-}c)^+/TiO_2(e^-)$.[25]

In this paper, we present a detailed study of the photosensitization of nanocrystalline metal oxide electrodes by ZnCyt-c and the application of such electrodes for the photogeneration of molecular hydrogen by visible light. A key issue in these studies is the increased spatial separation of the sensitizer (in this case the Zn−porphyrin species within the protein) from the electrode surface compared to the relatively intimate binding normally employed for the sensitization of such electrodes by molecular dyes. Consideration of the ZnCyt-c structure indicates that, even with an optimal binding orientation of the ZnCyt-c on the metal oxide surface, the porphyrin species is incorporated ~0.4 nm into a cavity within the protein interior.[26] Such interfacial electron-transfer kinetics between the redox sensitizor and the metal oxide electrode are expected to be slow relative to the analogous dye-sensitized systems, opening up the potential for not only singlet but also triplet state sensitization of the electrode. We employ transient absorption spectroscopy to interrogate these interfacial electron processes, and following determination of the conditions that result in optimum interfacial kinetics, we employ this redox-protein-sensitized film to achieve light-driven hydrogen production.

Experimental Procedures

Materials. All chemicals were obtained from Sigma-Aldrich Ltd. unless otherwise stated. Distilled water was demineralized to a resistivity of 10 MΩ cm. Horse-heart cytochrome *c* was obtained from Sigma-Aldrich Ltd. The preparation of free base horse-heart cytochrome *c* followed the method of Vanderkooi et al.[19] except for the use of pyridinium-bound poly(hydrogen fluoride) instead of gaseous hydrogen fluoride. The insertion of Zn(II) into the free base cytochrome and its purification were performed following Ye et al.,[22] yielding a ZnCyt-c solution with absorption maxima at 423, 549, and 585 nm, in good agreement with previous reports[19,22] and confirming the conformational integrity of the reconstituted protein. Fractions were collected with absorption maxima intensity ratios of A423/A549 >15.0 and A549/A585 < 2.0. Four micrometer thick nanocrystalline, mesoporous ZrO_2, TiO_2, and SnO_2 films were prepared on conducting glass substrates (TEC15 FTO, Hartford Glass, 15 Ohm-sq) as reported previously.[25,27] For hydrogen evolution studies, 8 μm, 1.5 cm^2 TiO_2 films were employed.

Protein Immobilization. A 25−30 μM solution of ZnCyt-c was prepared in 10 mM sodium phosphate (NaPi) buffer, pH 7. Prior to immobilization, a 1 cm^2 area of ZrO_2, TiO_2, or SnO_2 electrode on FTO glass was heated at 450 °C for 20 min to remove all the dirt and any adsorbed water. After cooling, the metal oxide electrodes were then immersed in ZnCyt-c solution at 4 °C for up to 1 week, with the resultant protein adsorption being monitored by the film optical absorbance. Possible contributions to the spectra from scattered light and absorption by the TiO_2, SnO_2, or ZrO_2 films were subtracted by the use of protein-free reference films. Prior to all spectroscopic measurements, films were rinsed with the buffer to remove nonimmobilized protein.

Light-Induced Transient Absorption Spectroscopy. Transient absorption data was conducted on sensitized electrodes as reported previously.[25] The ZnCyt-c-sensitized nanocrystalline films were placed in a quartz cuvette containing 10 mM NaPi buffer, pH 7, and degassed with argon for 30 min prior measurements, unless otherwise stated. For collection of transient absorption data, samples were excited at 549 nm employing a PTI GL-3300 nitrogen laser-pumped dye laser (pulse energy 40 μJ per cm^{-2}, repetition rate 0.8 Hz). The photoinduced change in film optical density was monitored using a 100 W tungsten lamp as a probe light, 20 nm bandwidth monochromators before and after the sample, home-built detection electronics, and a TDS-220 Tektronics DSO oscilloscope to digitize the data. Each transient decay was obtained from the average of ~25 laser excitation pulses.

Hydrogen Evolution from Water. For hydrogen evolution experiments, the 8 μm, 1.5 cm^2 TiO_2 film was internally coated with Pt by thermal pyrolysis of H_2PtCl_6 (Aldrich). A 0.5 M solution of H_2PtCl_6 in 2-propanol was spread over the film. Once dry, the slide was placed in a furnace at 400 °C for 10 min. To ensure the complete reduction of Pt salt to its metal form, the film was then dipped in 200 mM hydroquinone solution and then heated in an oven for 30 min at 50 °C,

(15) Astuti, Y.; Topoglidis, E.; Briscoe, P. B.; Fantuzzi, A.; Gilardi, G.; Durrant, J. R. *J. Am. Chem. Soc.* **2004**, *126*, 8001−8009.
(16) Astuti, Y.; Topoglidis, E.; Gilardi, G.; Durrant, J. R. *Bioelectrochemistry* **2004**, *63*, 55−59.
(17) Topoglidis, E.; Astuti, Y.; Duriaux, F.; Graetzel, M.; Durrant, J. R. *Langmuir* **2003**, *19*, 6894−6900.
(18) Topoglidis, E.; Discher, B. M.; Moser, C. C.; Dutton, P. L.; Durrant, J. R. *ChemBioChem* **2003**, *4*, 1332−1339.
(19) Vanderkooi, J. M.; Adar, F.; Erecinska, M. *Eur. J. Biochem.* **1976**, *64*, 381−387.
(20) Guo, L.-H.; Mukamel, S.; McLendon, G. *J. Am. Chem. Soc.* **1995**, *117*, 546−547.
(21) Logovinsky, V.; Kaposi, A. D.; Vanderkooi, J. M. *Biochim. Biophys. Acta* **1993**, *1161*, 149−160.
(22) Ye, S.; Shen, C.; Cotton, T. M.; Kostic, N. M. *J. Inorg. Biochem.* **1997**, *65*, 219−226.
(23) Pletneva, E. V.; Crnogorac, M. M.; Kostic, N. M. *J. Am. Chem. Soc.* **2002**, *124*, 14342−14354.
(24) Braun, M.; Atalick, S.; Guldi, D. M.; Lanig, H.; Brettreich, M.; Burghardt, S.; Hatzimarinaki, M.; Ravanelli, E.; Prato, M.; van Eldik, R.; Hirsch, A. *Chem.−Eur. J.* **2003**, *9*, 3867−3875.
(25) Topoglidis, E.; Campbell, C. J.; Palomares, E.; Durrant, J. R. *Chem. Commun.* **2002**, 1518−1519.
(26) Vanderkooi, J. M.; Glatz, P.; Casadei, J.; Woodrow, G. V. *Eur. J. Biochem.* **1980**, *110*, 189−196.
(27) Green, A. N. M.; Chandler, R. E.; Haque, S. A.; Nelson, J.; Durrant, J. R. *J. Phys. Chem. B* **2005**, *109*, 142−150.

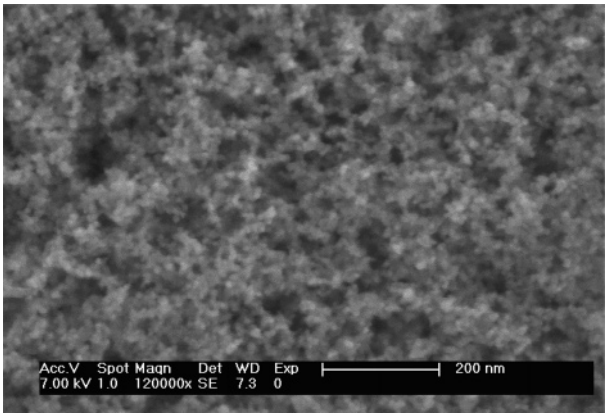

Figure 2. SEM image of a SnO_2 mesoporous nanocrystalline film.

followed by rinsing in water and heating in a furnace at 450 °C for 10 min.[28] Subsequent protein immobilization gave a ZnCyt-c loading of ~15 nmoles/cm^2. The resulting ZnCyt-c/TiO_2−Pt film was immersed in a transparent glass cuvette containing 5 mL of aqueous NaPi buffer solution (25 mM, pH = 5) and an electron donor, typically 10 mM EDTA. The system was degassed prior to hydrogen evolution measurements for 30 min with argon gas. The film was irradiated using an Osram 150 W tungsten halogen lamp with appropriat filters to avoid ultraviolet irradiation (λ > 475 nm), resulting in an irradiance at the film, measured with a calibrated silicon photodiode, of ~30 mW/cm^2. The formation of molecular hydrogen in the cuvette was measured using a H_2 electrode positioned above the solution. This electrode was connected to an Autolab PGSTAT12 potentiostat, and the calibration was conducted following literature methodologies.[29]

Results

Metal Oxide Film Characterization. The nanostructured, mesoporous metal oxide films employed all comprise transparent, porous networks of 15−20 nm nanoparticles. A typical scanning electron microscopy (SEM) image is shown in Figure 2. The pore sizes for the films, determined by Bruner−Emmet−Teller (BET) analysis, are 10−25 nm, sufficiently large for the protein molecules to diffuse throughout the porous structure. Film surfaces were determined by BET analyses to be 65, ~100, and 146 m^2/g for ZrO_2, SnO_2, and TiO_2 films respectively, corresponding to 300−800-fold enhancements of the film surface area relative to that of flat surfaces.

Protein Immobilization. The optical transparency of the metal oxide films allows the ZnCyt-c adsorption process to be monitored readily by eye as a pink coloration of the films or more quantitatively by UV−vis absorption spectroscopy. Figure 3 shows absorption spectra of 4 μm thick TiO_2, SnO_2, and ZrO_2 films following the immobilization of Zn−cytochrome *c*. The spectra show the characteristic heme absorption bands at 423 nm (Soret band) and 549 and 585 nm (Q-bands) for ZnCyt-c in good agreement with the solution spectra of this protein,[19] indicating that protein immobilization does not cause any detectable protein denaturation.[25] From the observed optical density of the resulting films and employing an extinction coefficient of 243 000 M^{-1} cm^{-1} at 423 nm for ZnCyt-c,[19] we obtain protein loadings of 3.1, 4.9, and 5.8 nanomoles cm^{-2} for the ZrO_2, SnO_2, and TiO_2 films, respectively. Assuming a cross-sectional area of ZnCyt-c of 700 Å,[14] these data indicates

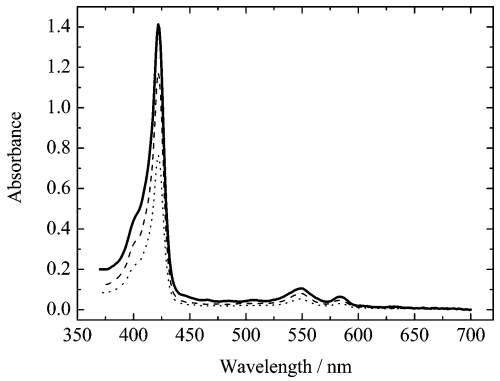

Figure 3. UV−vis absorption spectra for 4 μm thick ZnCyt-c/TiO_2 (—), ZnCyt-c/SnO_2 (- - -) and ZnCyt-c/ZrO_2 (• • •) electrodes. Contribution from absorption/scatter of the metal oxide films alone has been subtracted.

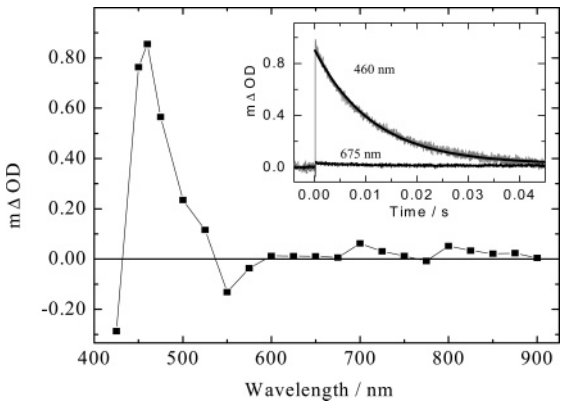

Figure 4. Absorption difference spectrum of ZnCyt-c/ZrO_2 films immersed in 10 mM NaPi buffer solution pH 7, collected at 1 ms after the pulsed laser excitation, assigned to the formation of the ZnCyt-c triplet state. The excitation wavelength was λ_{ex} = 549 nm (laser power = 40 μJ cm^{-2}, frequency = 0.8 Hz). The inset shows the corresponding decay dynamics of the transient absorption signal collected at probe wavelengths of 460 and 675 nm, along with (solid lines) monoexponential fits to these transients (lifetime of 12 ms).

approximately 0.7 ± 0.1 of monolayer coverage was achieved for each film. The protein coverage is similar to those we have reported previously for the immobilization of Fe(II)−Cyt-c on nanoporous TiO_2 electrodes.[14,18] Moreover, we have demonstrated that the binding of Cyt-c on this metal oxide is mainly electrostatic and therefore controlled by the buffer pH, the protein, the electrode surface charge, and the solution ionic strength.

Zn−Cytochrome *c* Triplet State, ^{3}ZnCyt-c. We consider first transient absorption data for ZnCyt-c/ZrO_2 films, as shown in Figure 4. In these films, electron injection from ZnCyt-c excited states into the metal oxide is not possible due to the high energy of the zirconia conduction band as confirmed by our previous time-resolved fluorescene studies of such films.[25] Rather, photogeneration of the ZnCyt-c excited singlet state (^{1}ZnCyt-c*) is expected, followed by rapid ($k_{isc} \sim 4 \times 10^{-8}$ s^{-1} [25,30]) intersystem crossing to the ZnCyt-c triplet state (^{3}ZnCyt-c). The transient spectrum shown in Figure 4 at 1 ms is in good agreement with this expectation, exhibiting a pronounced photoinduced absorption at 460 nm, assigned previously to ^{3}ZnCyt-c absorption.[31] Under anaerobic condition,

(28) Kraeutler, B.; Bard, A. J. *J. Am. Chem. Soc.* **1978**, *100*, 5985−5992.
(29) Hanus, F. J.; Carter, K. R.; Evans, H. J. In *Photosynthesis and Nitrogen Fixation (Part C)*; San Pietro, A., Ed.; Academic Press: London, 1980; Vol. 69, pp 731−740.
(30) Dixit, B. P. S. N.; Moy, V. T.; Vanderkooi, J. M. *Biochemistry* **1984**, *23*, 2103-2107.
(31) Elias, H.; Chou, M. H.; Winkler, J. R. *J. Am. Chem. Soc.* **1988**, *110*, 429−434.

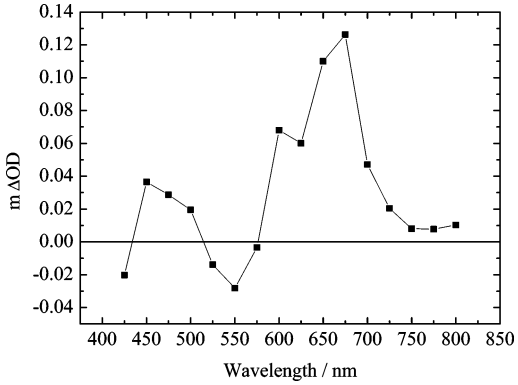

Figure 5. Transient absorption spectrum of ZnCyt-c/TiO_2 electrodes collected at 45 ms after the pulsed laser excitation. Other experimental conditions are the same as for Figure 4. This transient spectrum is assigned to the ZnCyt-c cation state generated by electron injection into the TiO_2 conduction band.

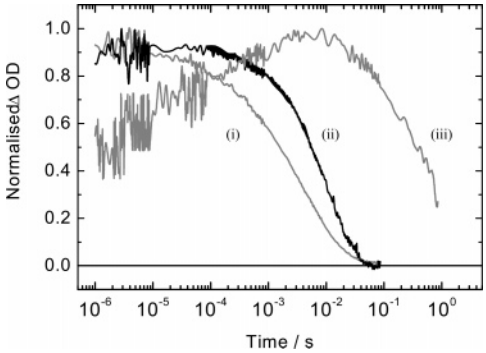

Figure 6. Normalized transients monitoring (i and ii) ^{3}ZnCyt-c absorption at 460 nm and (iii) absorption at 675 nm. Transients (i) and (iii) measured for ZnCyt-c/TiO_2 films, transient (ii) measured as control data for ZnCyt-c/ZrO_2 films. Electron injection from the photoexcited ZnCyt-c into the TiO_2 electrode is monitored both as an acceleration in the ^{3}ZnCyt-c absorption at 460 nm and the concomitant grow in of the ZnCyt-c^+ absorption at 675 nm. Other experimental conditions are the same as for Figure 4.

this 460 nm transient absorption exhibits a monoexponential decay with a lifetime of 12 ± 0.5 ms, again in good agreement with the previous solution studies of the ^{3}ZnCyt-c state,[19,30,31] accelerating to ~10 μs for air-equilibrated systems. The triplet quantum yield per absorbed photon (Φ_T) was determined from the magnitude of the absorption transient, assuming a triplet state molar absorption coefficient of 3.2×10^4 M^{-1} cm^{-1}, to be 0.7 ± 0.2, again consistent with previous solution studies.[30] We thus conclude that the immobilized ZnCyt-c exhibits a similar photophysics to previous solution studies of this protein including, in the absence of suitable electron accepting levels within the electrode, the photogeneration of a long-lived ^{3}ZnCyt-c triplet state.

Zn−Cytochrome *c* Cation, ZnCyt-c^+. We now consider the transient absorption spectrum obtained for ZnCyt-c/TiO_2 films, as shown in Figure 5. In this case, the relatively low conduction band edge of TiO_2 (~ −0.75 V versus Ag/AgCl at pH 7)[32] allows electron injection from the photoexcited ZnCyt-c into the metal oxide, consistent with our previous observations.[25] A long-lived transient signal is indeed observed, exhibiting a strong absorption maximum at 675 nm. Comparison of this spectrum to previous solution studies based on the oxidative quenching of the ^{3}ZnCyt-c excited state using quenchers such as Ru$(NH_3)_6^{3+}$,[31] plastocyanin,[33] or cytochrome oxidase[34] confirms the assignment of this 675 nm band to absorption of oxidized ZnCyt-c (ZnCyt-c^+). Assuming an extinction coefficient of 1.4×10^{-4} M^{-1} cm^{-1} for the ZnCyt-c^+ at 675 nm,[31] the quantum yield for cation formation (Φ_c) is estimated as approximately 0.25.

Electron-Transfer Kinetics. Figure 6compares transients measured at 460 nm, the triplet absorption maximum for ZnCyt-c/TiO_2 (trace i) and ZnCyt-c/ZrO_2 (trace ii) films. It is apparent that the decay dynamics of the ^{3}ZnCyt-c absorption at 460 nm exhibit a 4-fold acceleration on the TiO_2 electrode, consistent with efficient quenching of this state by electron injection into the TiO_2 conduction band. Trace iii shows the transient signal at 675 nm, corresponding to the ZnCyt-c^+ absorption maximum, for the ZnCyt-c/TiO_2 film. The data are plotted on a logarithmic time scale to show both the grow in and decay of the transient signal. It is apparent that the grow in is biphasic, an instrument limited rise (<1 μs) followed by a slower rise on the microsecond time scale. The instrument response limited rise is assigned to both weak triplet state absorption at this wavelength[35] and to electron injection on the nanosecond time scale from the ZnCyt-c singlet state, consistent with our previous time-resolved emission studies of analogous films.[17] The slower, microsecond rise is assigned to electron injection from the ^{3}ZnCyt-c, consistent with the accelerated 460 nm decay dynamics shown in trace i of Figure 6. The slower injection dynamics for the ^{3}ZnCyt-c relative to the ^{1}ZnCyt-c* excited states are attributed to the lower energy of the ^{3}ZnCyt-c reducing the density of TiO_2 acceptor states available for electron injection.

Further evidence for significant triplet state electron injection comes from a comparison of data collected under aerobic rather than anaerobic conditions, as shown in Figure 7. Aerobic conditions result in a 1000-fold acceleration of the ^{3}ZnCyt-c absorption decay dynamics monitored at 460 nm (Figure 7a) and almost complete quenching of ZnCyt-c^+ transient absorption at 675 nm (Figure 7b), consistent with ZnCyt-c^+ formation being dominated by electron injection from the ZnCyt-c triplet state.

The ZnCyt-c^+ absorption observed for the ZnCyt-c/TiO_2 film exhibited very slow decay dynamics, with a decay time of 0.4 ± 0.1 s (Figure 6 trace iii), consistent with our previous studies of analogous films. These decay dynamics are assigned to charge recombination of injected electrons with the ZnCyt-c^+ species. The slow time scale of these recombination dynamics relative to those typically observed for molecular sensitizers adsorbed to such TiO_2 films is attributed to a large physical separation of the ZnCyt-c porphyrin macrocycle from the TiO_2 surface.[36]

Optimization of Electron-Transfer Kinetics. The charge separation efficiency and lifetime of the charge-separated state were monitored as a function metal oxide employed and solution pH. Figure 8 shows typical absorption transients monitoring the formation and decay of the ZnCyt-c^+ cation at 675 nm for ZnCyt-c-sensitized TiO_2 and SnO_2 films at pH 5 and 7. The ZnCyt-c^+ cation yield, as monitored by the maximal amplitude

(32) Hagfeldt, A.; Graetzel, M. *Chem. Rev.* **1995**, *95*, 49−68.
(33) Zhou, J. S.; Kostic, N. M. *J. Am. Chem. Soc.* **1991**, *113*, 7040−7042.
(34) Brzezinski, P.; Sundahl, M.; Aedelroth, P.; Wilson, M. T.; El-Agez, B.; Wittung, P.; Malmstroem, B. G. *Biophys. Chem.* **1995**, *54*, 191−197.
(35) Consideration of the triplet state spectrum shown in Figure 4 and the relative signal magnitudes at 460 and 675 nm observed for the ZnCyt-c/TiO_2 indicate approximately 90 ± 5% of this initial absorption increase derives from ^{3}ZnCyt-c absorption.
(36) Haque, S. A.; Handa, S.; Peter, K.; Palomares, E.; Thelakkat, M.; Durrant, J. R. *Angew. Chem.*, in press.

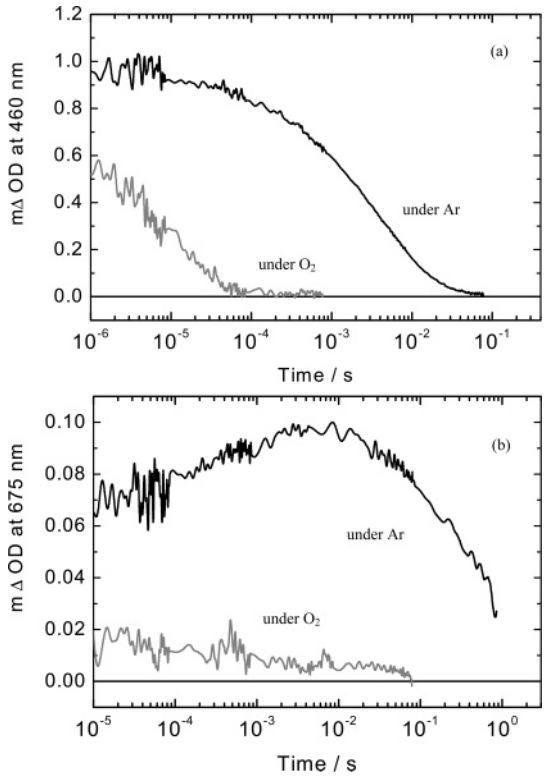

Figure 7. Transients monitoring (a) ^{3}ZnCyt-c absorption at 460 nm and (b) ZnCyt-c$^+$ absorption at 675 nm, determined under oxygen and argon atmospheres for ZnCyt-c/TiO_2 films.

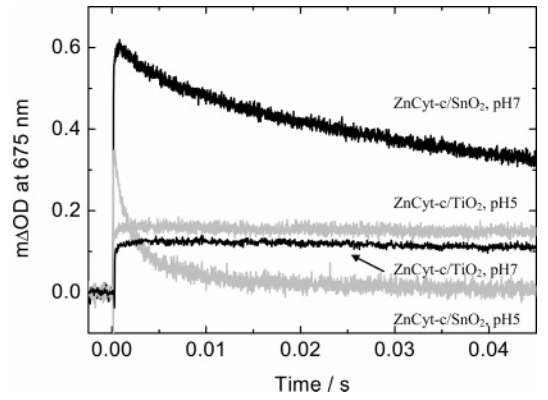

Figure 8. Transient signals monitoring ZnCyt-c$^+$ absorption at 675 nm, following pulsed laser excitation of ZnCyt-c immobilized on TiO_2 and SnO_2 electrodes immersed in 10 mM NaPi buffer pH 7 and pH 5.

of the transient signal, was found to be greater for SnO_2 films ($\Phi_c \sim 1 \pm 0.1$), consistent with the low-energy conduction band of this metal oxide[32] providing a greater energetic driving force for electron injection. Similarly a higher yield ($\Phi_c \sim 0.32 \pm 0.05$) was observed at pH 5 relative to pH 7, consistent with the well-established Nernstian dependence of the TiO_2 conduction band[32,37] resulting in, at more acidic pHs, a lower energy conduction band and therefore again greater energetic driving for electron injection. The advantage of SnO_2 films in terms of ZnCyt-c$^+$ yield is, however, offset by much faster charge recombination dynamics of the injected electrons with the ZnCyt-c$^+$ (half-lifetime of 79 ms at pH 7) compared to those of the TiO_2 films resulting in greatly accelerated electron

(37) Shinohara, H.; Graetzel, M.; Vlachopoulos, N.; Aizawa, M. *Bioelectrochem. Bioenerg.* **1991**, *26*, 307−320.

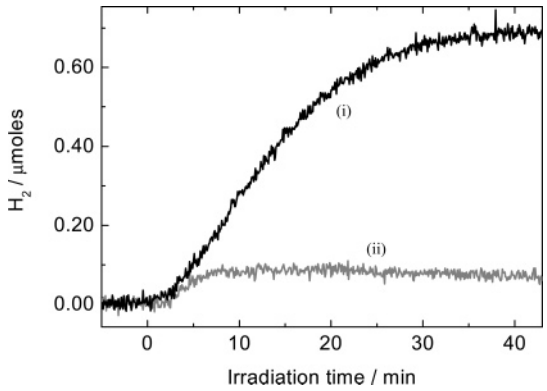

Figure 9. Kinetics for the hydrogen formation observed following the white light (λ > 475 nm) illumination of (i) a ZnCyt-c/TiO_2−Pt electrode and (ii) a TiO_2−Pt electrode control electrode immersed in a transparent glass cuvette containing aqueous 5 mL NaPi buffer solution (25 mM, pH = 5) and 10 mM EDTA as a sacrificial electron donor. Hydrogen evolution was measured with an electrochemical hydrogen electrode under anaerobic conditions.

transport dynamics with in the SnO_2 nanoparticles. These accelerated recombination dynamics are consistent with our previous studies of charge recombination in dye-sensitized TiO_2 and SnO_2 films[27] and assigned primarily to reduced electron trapping within the SnO_2 film. On the basis of these studies, TiO_2 films at pH 5 were selected for hydrogen evolution studies, as detailed below.

Hydrogen Evolution from Water. Having shown long-lived photogenerated charge separation resulting from the sensitization of a nanocrystalline TiO_2 film with ZnCyt-c, we now turn to consideration of the ability of this artificial photosystem to generate molecular hydrogen. A platinum catalyst was loaded on the nanocrytalline TiO_2 film before ZnCyt-c immobilization to catalyze the reduction of protons to molecular hydrogen by electrons photoinjected into the TiO_2 electrode. EDTA was added to the immersion solution to function as a sacrificial electron donor, and the solution pH was maintained at pH 5 using 25 mM NaPi buffer. The absorption spectrum of the immobilized ZnCyt-c was independent of the addition of EDTA to the buffer, indicating that the EDTA did not result in any significant degradation of immobilized protein. Figure 9 show the time dependence of photoinduced hydrogen evolution observed during white (λ > 475 nm) light radiation of the sample by a hydrogen electrode. Control data with TiO_2−Pt films alone showed only minor H_2 evolution activity (Figure 9, trace ii). An ∼10-fold increase in H_2 evolution was observed upon using the ZnCyt-c/TiO_2−Pt electrode (trace i). Hydrogen generation was only observed in the presence of illumination, consistent with it resulting from optical excitation of the sensitized photoelectode. The concentration of hydrogen in the photoelectrochemical cell reached steady state after 40 min of continuous illumination, most probably due to the increased hydrogen consumption by the hydrogen electrode (and hydrogen leakage from the cell) matching the rate of photochemical hydrogen production. Subsequent incubation of the cell in the dark (allowing the hydrogen concentration to fall to approximately zero) followed by repeated illumination resulted in almost complete recovery of photochemical hydrogen production, indicating good photochemical stability of the photoelectrode. We further note that the number of moles of molecular H_2 produced exceeds the moles of ZnCyt present by almost 2

orders of magnitude, clearly indicating that the ZnCyt is not functioning as a "consumable photosensitizer". The rate of H_2 evolution was estimated to be 17 nmol/min for the first 20 min of illumination. Assuming two electrons per hydrogen molecule released, this corresponds to a quantum yield of hydrogen production of 10 ± 5% per one absorbed photon.[38,39] This indicates a quantum yield for hydrogen production per two photons absorbed (as the generation of one molecular of hydrogen requires two electrons) of 20 ± 10%, which is of the same order of magnitude as the quantum yield of ZnCyt-c^+ cations determined from our transient optical experiments and indicates remarkably efficient photoreduction of protons to molecular hydrogen by our photoelectrode with only limited recombination losses.

Discussion

We have demonstrated a remarkably simple photoelectrode for the photogeneration of molecular hydrogen. Mesoporous, nanocrystalline metal oxide electrodes are now well established as robust, nontoxic photoelectrodes for a range of photocatalytic and energy conversion systems. The addition of platinum catalysts for proton reduction to molecular hydrogen is well documented and has previously been shown to be highly effective catalysts.[40−42] ZnCyt-c is readily prepared from natural Cyt-c and is a robust and well-characterized redox protein. Protein adsorption achieving almost monolayer coverage of the mesoporous metal oxide films is achieved by simple immersion of the unsensitized film in an appropriate buffer solution.[15−17] Following these simple procedures, visible light photogeneration of molecular hydrogen is achievable with a quantum yield of ~10 ± 5% per one photon absorbed, comparable to the best light photoelectrodes reported to date.[43−47]

There are clearly significant limitations to the study reported here. Most obviously, the photosystem developed does not oxidize water to molecular oxygen but rather requires the addition of a sacrificial electron donor (in common with most other hydrogen photogeneration systems reported to date).[41,48,49] Moreover, there are clearly issues of efficiency optimization and photochemical stability, which remain to be addressed. We have, however, demonstrated a potentially generic strategy for the interfacing of light-absorbing redox proteins with a nanostructured, inorganic hydrogen generation catalysts. As such, it is possible to envisage the incorporation of further light-absorbing pigments and oxidation catalysts with the sensitizing protein, employing either existing natural pigment protein complexes or artificial protein maquettes, which could lead to development of an innovative and fully regenerative artificial photosynthetic system.

Our studies reported elsewhere have demonstrated that protein immobilization on mesoporous metal oxide electrodes is not limited to Cyt-c but can be readily achieved for a wide range of natural and synthetic redox proteins and, moreover, for larger water soluble enzymes including cytochrome *c* peroxidase and the catalytic domain of cytochrome P450 BM3.[15−18] The hydrophilic nature of the metal oxide surfaces appears to favor protein adsorption without inducing denaturation; indeed long-term stability studies with Cyt-c have demonstrated an improved conformation stability of this protein adsorbed to mesoporous TiO_2 electrodes compared to the same protein suspended in aqueous buffer solutions.[14]

In addition to our observation of hydrogen photogeneration, our observation of triplet state sensitization of the nanocrystalline metal oxide electrodes is of particular interest. Previous studies of light-induced electron injection into mesoporous metal oxide electrodes have typically focused on achieving strong electronic coupling between the metal oxide nanoparticles and the sensitizing species, this resulting in ultrafast electron injection into the metal oxide conduction band.[6] However, as we have discussed in detail elsewhere, such strong electronic coupling tends to have the disadvantage of resulting in relatively fast charge recombination dynamics between the injected electrons and sensitizer cations, which can result in significant efficiency losses of overall energy conversion.[36] In the system reported here, the protein matrix acts as a physical spacer between the sensitizer molecule (the Zn−porphyrin) and the nanoparticle surface. As such, electron injection from the singlet state of the sensitizer, although possible,[25] is likely to be less efficient. We demonstrate here an alternative electron injection pathway on relatively slow (microsecond) time scales proceeding from the sensitizer triplet state. Triplet state sensitization from this sensitizer is favored by the high S_1 to T_1 intersystem crossing efficiency of ZnCyt-c (measured as 0.9 in aqueous solution),[30] long triplet state lifetime (12 ms on inert electrodes), and relatively small energy splitting between the S_1 and T_1 states (350 meV[19]). This sensitization pathway has the advantage of requiring only relatively weak electronic coupling between the sensitizer and the electrode surface, resulting in concomitantly slow interfacial charge recombination dynamics, as observed here, and thereby facilitating efficient energy conversion.

It is striking that the quantum yield for hydrogen evolution reported here is higher than that reported previously for analogous dye-sensitized nanocrystalline TiO_2 photoelectrodes.[43] Most probably, the high efficiency we report here is associated with the long lifetime (0.4 s) of the $TiO_2(e^-)$/ZnCyt-c^+ charge-separated state, along with the reasonable charge separation quantum efficiency. These promising results confirm the potential of redox proteins to achieve efficient sensitization of nanocrystalline metal oxide films for light-driven hydrogen evolution. Extensions to this study employing synthetic redox proteins selected to optimize electron-transfer function are currently in progress and will hopefully lead to further improvements in device efficiency and, ultimately, potentially to the

(38) Herein we define the quantum yield as the ratio of the initial rate of hydrogen production to the rate of two photons absorbed by the Q-bands of immobilized ZnCyt-c. Taking account of sample absorption at wavelengths longer than the 475 nm cut off filter (absorption maximum of 0.25 at 549 nm), the flux of absorbed photons was estimated as 0.7 mW cm^{-2}.

(39) Serpone, N.; Salinaro, A. *Pure Appl. Chem.* **1999**, *71*, 303−320.
(40) Borgarello, E.; Kiwi, J.; Pelizzetti, E.; Visca, M.; Graetzel, M. *J. Am. Chem. Soc.* **1981**, *103*, 6324−6329.
(41) Jiang, D.-L.; Choi, C.-K.; Honda, K.; Li, W.-S.; Yuzawa, T.; Aida, T. *J. Am. Chem. Soc.* **2004**, *126*, 12084−12089.
(42) Hinnemann, B.; Moses, P. G.; Bonde, J.; Jorgensen, K. P.; Nielsen, J. H.; Horch, S.; Chorkendorff, I.; Norskov, J. K. *J. Am. Chem. Soc.* **2005**, *127*, 5308−5309.
(43) Kim, H. G.; Hwang, D. W.; Kim, J.; Kim, Y. G.; Lee, J. S. *Chem. Commun.* **1999**, 1077−1078.
(44) Abe, R.; Sayama, K.; Arakawa, H. *J. Photochem. Photobiol., A* **2004**, *166*, 115−122.
(45) Abe, R.; Hara, K.; Sayama, K.; Domen, K.; Arakawa, H. *J. Photochem. Photobiol., A* **2000**, *137*, 63−69.
(46) Aroutiounian, V. M.; Arakelyan, V. M.; Shahnazaryan, G. E. *Sol. Energy* **2005**, *78*, 581−592.
(47) Mor, G. K.; Shankar, K.; Paulose, M.; Varghese, O. K.; Grimes, C. A. *Nano Lett.* **2005**, *5*, 191−195.
(48) Saiki, Y.; Amao, Y. *Int. J. Hydrogen Energy* **2004**, *29*, 695−699.
(49) Evans, B. R.; O'Neill, H. M.; Hutchens, S. A.; Bruce, B. D.; Greenbaum, E. *Nano Lett.* **2004**, *4*, 1815−1819.

coupling of such redox chemistry to enzymatic action such as water oxidation.

Acknowledgment. We gratefully acknowledge the financial support of the BBSRC and EPSRC and thank Chris Moser and Leslie Dutton, Pennsylvania State University, for helpful discussions, Alex Green for assistance with metal oxide paste preparation, and Narukuni Hirata for assistance with the transient studies. E.P. would like to acknowledge the financial support from the European Union (Marie Curie European Fellowship Contract No. HPMF-CT-2002-0144).

JA0533444